

Hydrothermal synthesis and structure of $[(C_4N_2H_{12})_3][P_2Mo_5O_{23}] \cdot H_2O$ and $[(C_3N_2H_{12})_3][P_2Mo_5O_{23}] \cdot 4H_2O$

S V GANESAN and SRINIVASAN NATARAJAN*

Framework Solids Laboratory, Solid State and Structural Chemistry Unit, Indian Institute of Science, Bangalore 560 012, India
e-mail: snatarajan@sscu.iisc.ernet.in

MS received 4 December 2004; revised 24 January 2005

Abstract. Two new compounds, $[(C_4N_2H_{12})_3][P_2Mo_5O_{23}] \cdot H_2O$, **I**, and $[(C_3N_2H_{12})_3][P_2Mo_5O_{23}] \cdot 4H_2O$, **II**, have been prepared employing hydrothermal methods in the presence of aliphatic organic amine molecules. Both the compounds possess the same polyoxoanion, pentamolybdatobisphosphate, $(P_2Mo_5O_{23})^{6-}$. The anions consist of a ring of five MoO_6 distorted octahedra with four edge connections and one corner connection. The phosphate groups cap the pentamolybdate ring anion on either side. The anion is stabilized by strong hydrogen bonds involving the hydrogen atoms of the amine molecules and the oxygen atoms of the polyoxoanion and water molecules. Crystal data: **I**, monoclinic, space group = $P2_1/n$ (no. 14), mol. wt. = 1192·1, $a = 9\cdot4180(1)$, $b = 18\cdot1972(3)$, $c = 19\cdot4509(1)$ Å, $\mathbf{b} = 103\cdot722(1)^\circ$, $V = 3238\cdot37(7)$ Å³, $Z = 4$; **II**, triclinic, space group = $P\bar{1}$ (no. 2), mol. wt. = 1210·1, $a = 9\cdot5617(9)$, $b = 13\cdot3393(12)$, $c = 13\cdot7637(12)$ Å, $\mathbf{a} = 88\cdot735(1)$, $\mathbf{b} = 75\cdot68(1)$, $\mathbf{g} = 87\cdot484(2)^\circ$, $V = 1699\cdot2(3)$ Å³.

Keywords. Pentamolybdatobisphosphate; cluster compounds; hydrogen bond; hydrothermal synthesis; crystal structure.

1. Introduction

Polyoxoanions of varying compositions and structures have been prepared and characterized.¹ Polyoxometallates find many applications in the areas of catalysis, medicine and materials science.^{1–4} Though polyoxometallates of many shapes and sizes have been prepared and characterized, their formation is still not well understood. The path breaking research by Muller and coworkers has resulted in the isolation of many novel polyoxomolybdates with very large clusters.⁵ Of the many polyoxomolybdates that have been prepared, the Strandberg anion $[H_xP_2Mo_5O_{23}]^{(6-x)}$,^{6–9} the Keggin anion $[PMo_{12}O_{40}]^{3-}$,^{10,11} and the Wells–Dawson anion, $[P_2Mo_{18}O_{62}]^{6-}$ appear to be well known.^{12,13} In addition, a large number of molybdenum containing compounds with a variety of structures and compositions have also been prepared and characterized.¹⁴ Synthesis and structure of the pentamolybdo (Mo_5) compounds stabilized by phosphate,^{6,16,17} phosphonate,^{18–20} phosphite⁷ and phosphonocarboxylates²¹ have already been reported. We have been interested in assembling many of these

polyoxomolybdates into extended networks using suitable linkers. To this end, we have recently reported the assembly of **b**-octamolybdates into extended structures.²² In continuation of the same theme, we have now isolated two pentamolybdatobisphosphates, $[(C_4N_2H_{12})_3][P_2Mo_5O_{23}] \cdot H_2O$, **I**, and $[(C_3N_2H_{12})_3][P_2Mo_5O_{23}] \cdot 4H_2O$, **II**, in the presence of piperazine and 1,2-diaminopropane, respectively. In this paper, we present the synthesis, structure and characterization of both these compounds.

2. Experimental

2.1 Synthesis and initial characterization

The two compounds, **I** and **II**, were synthesized employing hydrothermal methods in the presence of piperazine (PIP) and 1,2-diaminopropane (1,2-DAP) respectively. In a typical synthesis, for **I**, 0·324 g of $FeCl_2 \cdot 4H_2O$ (1·62 mM) was dissolved in 10 ml of water (555 mM). To this, 0·44 ml of H_3PO_4 (85%) (6 mM), 0·471 g of H_2MoO_4 (2·9 mM) and 0·303 g of H_3BO_3 (4·0 mM) were added sequentially. Finally, 0·844 g of piperazine (PIP) (9·7 mM) was added and the mixture was homogenized at room temperature

*For correspondence

for about 1 h. The final reaction mixture with the composition, $0.5\text{FeCl}_2 \cdot 4\text{H}_2\text{O} : 2\text{H}_3\text{PO}_4 : 1\text{H}_2\text{MoO}_4 : 1.5\text{H}_3\text{BO}_3 : 3\text{PIP} : 170\text{H}_2\text{O}$, was sealed in a PTFE-lined stainless steel autoclave (23 ml capacity) and heated at 125°C for 96 h. The initial pH of the reaction mixture was ~8 and did not show appreciable change after the completion of the reaction. The resulting product containing colourless hexagonal isometric single crystals admixed with dark-coloured powder were filtered, washed with deionized water and dried at ambient conditions. The yield of the single crystalline product was ~30% based on Mo. Compound **II** was prepared employing similar molar composition and synthetic procedure, but by using 1,2-DAP in place of piperazine, resulting in large quantities of fine needle-like colourless single crystals and dark-coloured powder (yield of the single crystals ~25% based on Mo). The initial and final pH of the reaction mixture was ~6. The crystals, in both the cases, could be easily separated from the bulk using an optical microscope and were used for all the characterization purposes. We have not been able to characterize the black powder, as it does not correspond to any known solid including the starting materials. The exact role of the ferrous chloride and boric acid in the mixture is not clear to us, but our efforts to synthesize **I** and **II** in their absence were not successful. Similar behaviour has also been encountered in many preparations employing hydrothermal technique.²² An EDAX analysis on many single crystals indicated a Mo/P ratio of 5:2 for both the compounds. Results of the elemental analysis of the bulk product are also consistent with the stoichiometry. Anal. Found: C, 11.95; H, 3.18; N, 6.98%; Calcd: C, 12.09; H, 3.21; N, 7.05% for **I** and C, 8.91; H, 3.61; N, 6.82%; Calcd: C, 8.93; H, 3.66; N, 6.95% for **II**.

Initial characterizations for both the compounds were carried out using powder X-ray diffraction (XRD), IR, and photoluminescence studies. Satisfactory thermogravimetric analysis (TGA) could not be performed as the sample was thrown out of the crucible, possibly due to the molecular nature of the samples. Powder XRD patterns indicated that the products were new materials; the patterns were entirely consistent with the structures determined using single-crystal X-ray diffraction. A least-squares fit of the powder XRD ($\text{CuK}\alpha$ radiation) lines, using the hkl indices generated from single-crystal X-ray data, gave the following cell, for **I**, $a = 9.410(4)$, $b = 18.191(4)$, $c = 19.443(6)$ Å, $\beta = 103.479(5)^\circ$ and for **II**, $a = 9.531(4)$, $b = 13.304(6)$, $c = 13.806(3)$ Å, $\alpha =$

$88.69(3)$, $b = 75.59(4)$, $g = 87.52(4)^\circ$, which are in reasonable agreement with that determined using the single crystal XRD. Typical powder X-ray data along with the simulated one for **I** is presented in figure 1.

Infrared (IR) spectra of **I**–**II** were recorded on Bruker IFS-66V/S equipment in the range 400 – 4000 cm^{-1} using the KBr pellet method. The IR spectra of the two compounds showed typical peaks, with very little differences between the spectra. Strong absorption bands for N–H and O–H bending and stretching vibrations are observed, in addition to the Mo–O bridging and terminal bonds. The various bands for **I**: 3573.5 , 3418.6 cm^{-1} – $\text{n}_{\text{as}}(\text{OH})$, 3233.3 cm^{-1} – $\text{n}_{\text{as}}(\text{N–H})$, 3005.5 cm^{-1} – $\text{n}_{\text{as}}(\text{C–H})$, 2957.9 cm^{-1} – $\text{n}_{\text{s}}(\text{C–H})$, 1612.9 cm^{-1} – $\text{d}_{\text{as}}(\text{N–H})$, 1592.9 cm^{-1} – $\text{d}_{\text{s}}(\text{N–H})$, 1458.8 cm^{-1} – $\text{d}_{\text{as}}(\text{C–H})$, 1396.5 cm^{-1} – $\text{d}_{\text{s}}(\text{C–H})$, 1303.8 cm^{-1} – $\text{d}(\text{O–H})$, 1220.9 cm^{-1} – $\text{n}_{\text{as}}(\text{C–N})$, 1189.8 cm^{-1} – $\text{n}_{\text{s}}(\text{C–N})$, 1053.2 , 1016.3 , 1003.7 cm^{-1} – $\text{n}(\text{P–O})$, 971.1 , 948.5 , 899.3 , 873.6 , 844.3 cm^{-1} – $\text{n}(\text{Mo–O}_{\text{terminal}})$, 660.3 , 591.7 cm^{-1} – $\text{n}(\text{Mo–O}_{\text{bridging}})$; for **II**: 3456.3 cm^{-1} – $\text{n}_{\text{as}}(\text{OH})$, 3250 cm^{-1} – $\text{n}_{\text{as}}(\text{N–H})$, 3002.7 cm^{-1} – $\text{n}_{\text{as}}(\text{C–H})$,

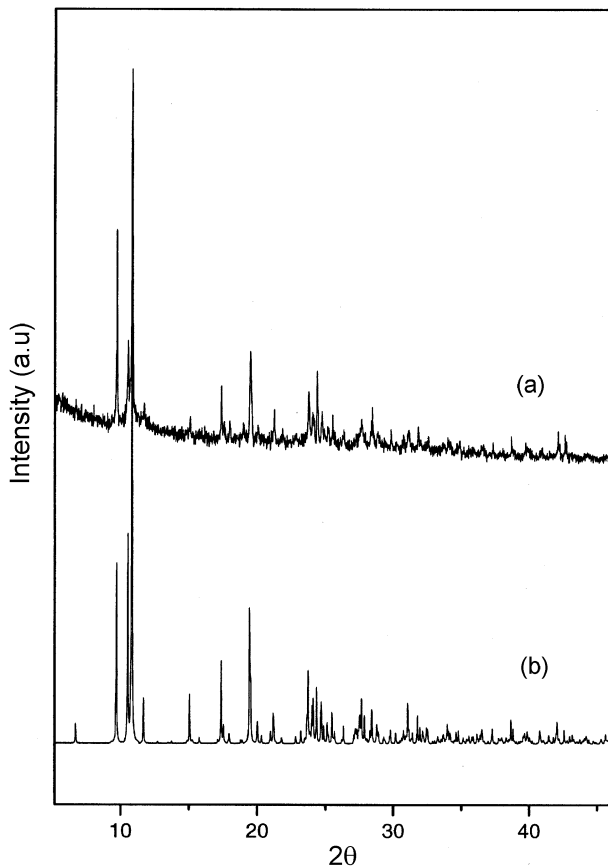


Figure 1. Powder XRD pattern ($\text{CuK}\alpha$) of $[(\text{C}_4\text{N}_2\text{H}_{12})_3[\text{P}_2\text{Mo}_5\text{O}_{23}]\cdot\text{H}_2\text{O}$, **I**. (a) Experimental and (b) simulated.

2967.4 cm^{-1} – \mathbf{n}_s (C–H), 1632.4 cm^{-1} – \mathbf{d}_{as} (N–H), 1599.9 cm^{-1} – \mathbf{d}_s (N–H), 1410.5 cm^{-1} – \mathbf{d}_{as} (C–H), 1391.5 cm^{-1} – \mathbf{d}_s (C–H), 1324.9 cm^{-1} – \mathbf{d} (O–H), 1210.2 cm^{-1} – \mathbf{n}_{as} (C–N), 1181.4 cm^{-1} – \mathbf{n}_s (C–N), 1046 , 1024.5 , 1006.4 cm^{-1} – \mathbf{n} (P–O), 921.5 , 883.3 , 808.4 cm^{-1} – \mathbf{n} (Mo–O_{terminal}), 690.2 , 658.1 cm^{-1} – \mathbf{n} (Mo–O_{bridging}). IR spectra in the region of 1750 – 500 cm^{-1} are given in figure 2.

Photoluminescence studies have been carried out on a Perkin–Elmer fluorescence spectrometer (model no. LS-55) equipped with a xenon lamp source and single monochromator on the emission side. Samples were excited using an excitation wavelength of 240 nm , and a weak emission was observed at 380 nm for both the samples. According to Peng,²³ the luminescent mechanism for the framework solids has not been unambiguously known. In many framework solids synthesized using organic amine cations, the photoluminescence could be due to the highly negatively charged inorganic framework and presence of protonated guest amine molecules. The

present compounds, **I** and **II**, satisfies these two criteria and the weak photoluminescence observed could be attributed to the negative charge on the $[\text{P}_2\text{Mo}_5\text{O}_{23}]^{6-}$ and the doubly protonated amine molecules.

2.2 Single crystal structure solution

A suitable single crystal of each compound was carefully selected under a polarizing microscope and glued to a thin glass fiber with cyanoacrylate (super glue) adhesive. Crystal structure determination by X-ray diffraction was performed on a Siemen's SMART-CCD diffractometer equipped with a normal focus, 2.4 kW sealed-tube X-ray source (MoK α radiation, $\lambda = 0.71073\text{ \AA}$) operating at 50 kV and 40 mA . Hemispheres of intensity data were collected at room temperature in 1321 frames with w scans (width of 0.30° and exposure time of 10 s per frame) in the $2q$ ranges 3 to 46.5° . Pertinent experimental details for the structure determinations of **I** and **II** are presented in table 1.

An absorption correction was applied using SADABS program.²⁴ The structures were solved by direct methods and, in each case, a sufficient fragment of the structure was revealed to enable the remainder of the non-hydrogen atoms to be located from difference Fourier maps and the refinements to proceed to $R < 10\%$. All the hydrogen positions for both the compounds were initially located in the difference map and for the final refinement the hydrogen atoms were placed geometrically and held in the riding mode. The last cycles of refinement included atomic positions for all the atoms, anisotropic thermal parameters for all non-hydrogen atoms, isotropic thermal parameters for all the hydrogen atoms. Full-matrix least-squares refinement against $|F|^2$ was carried out using the SHELXTL-PLUS suite of programs.²⁵ Details of the final refinement are given in table 1.

3. Results and discussion

Both **I** and **II** have oxopentamolybdate octahedral rings capped on either side by phosphate tetrahedra. For **I**, the asymmetric unit consists of 49 non-hydrogen atoms of which 30 belong to the pentamolybdate bisphosphate and the remaining belong to one molecule of water and three molecules of doubly protonated piperazine molecules (figure 3a). Mo–O distances are in the range $1.701(4)$ – $2.358(4)\text{ \AA}$ (average 1.978 \AA). Mo–O distances can be divided into

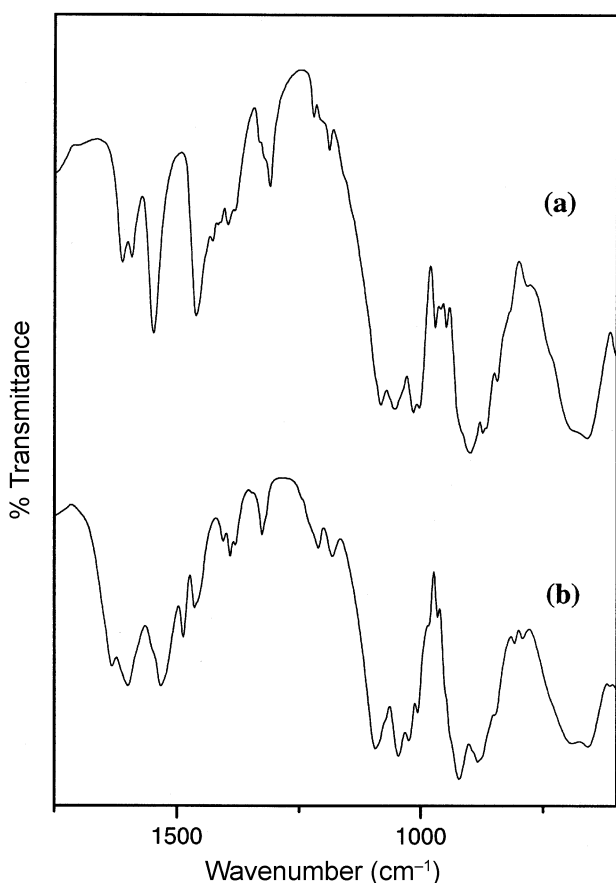


Figure 2. Infrared spectra of (a) $[(\text{C}_4\text{N}_2\text{H}_{12})_3][\text{P}_2\text{Mo}_5\text{O}_{23}]\cdot\text{H}_2\text{O}$, **I**, and (b) $[(\text{C}_3\text{N}_2\text{H}_{12})_3][\text{P}_2\text{Mo}_5\text{O}_{23}]\cdot 4\text{H}_2\text{O}$, **II**, showing characteristic bands.

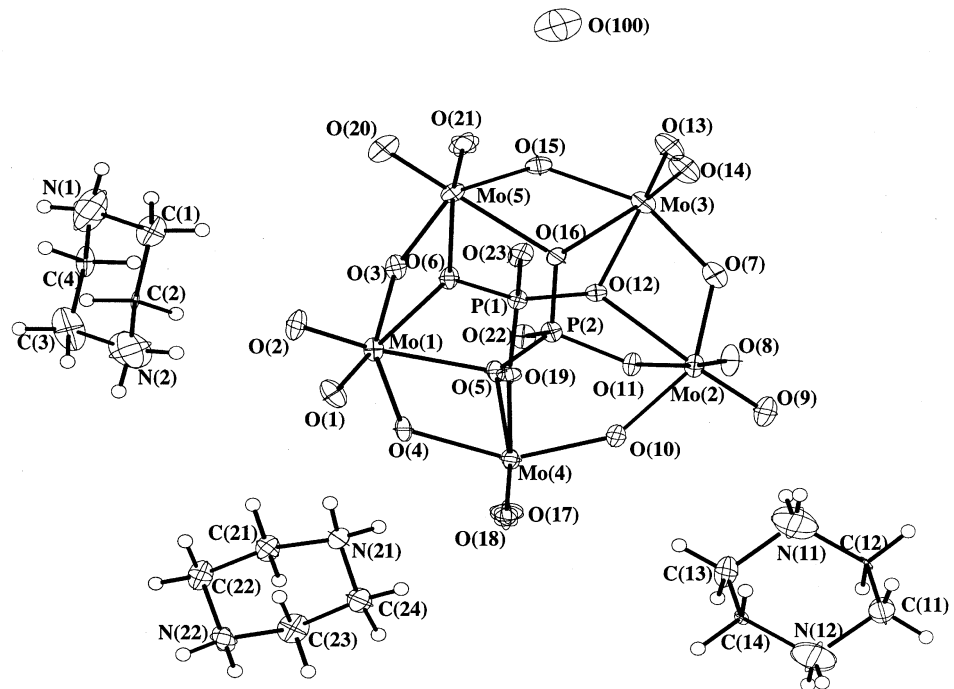


Figure 3. ORTEP diagram showing the asymmetric unit in $[(\text{C}_4\text{N}_2\text{H}_{12})_3][\text{P}_2\text{Mo}_5\text{O}_{23}]\cdot\text{H}_2\text{O}$, **I**. Thermal ellipsoids are given at 50% probability.

Table 1. Crystal data and structure refinement parameters for **I** $[(\text{C}_4\text{N}_2\text{H}_{12})_3][\text{P}_2\text{Mo}_5\text{O}_{23}]\cdot\text{H}_2\text{O}$, and **II** $[(\text{C}_3\text{N}_2\text{H}_{12})_3][\text{P}_2\text{Mo}_5\text{O}_{23}]\cdot 4\text{H}_2\text{O}$.

Structure parameter	I	II
Empirical formula	$\text{C}_{12}\text{H}_{38}\text{Mo}_5\text{N}_6\text{O}_{24}\text{P}_2$	$\text{C}_{9}\text{H}_{44}\text{Mo}_5\text{N}_6\text{O}_{27}\text{P}_2$
Formula weight	1192.12	1210.14
Crystal system	Monoclinic	Triclinic
Space group	$P2_1/n$ (no. 14)	$P\bar{1}$ (no. 2)
Crystal size (mm)	$0.32 \times 0.20 \times 0.20$	$0.20 \times 0.08 \times 0.08$
<i>a</i> (Å)	9.4180(1)	9.5617(9)
<i>b</i> (Å)	18.1972(3)	13.3393(12)
<i>c</i> (Å)	19.4509(1)	13.7637(12)
<i>a</i> (°)	90.0	88.735(1)
<i>b</i> (°)	103.722(1)	75.68(1)
<i>g</i> (°)	90.0	87.483(2)
Volume (Å ³)	3238.37(7)	1699.2(3)
<i>Z</i>	4	2
<i>r</i> _{calc} (g cm ⁻³)	2.445	2.365
<i>m</i> (mm ⁻¹)	2.085	1.995
<i>q</i> range	1.55–23.29	1.53–23.28
Total data collected	13634	7150
Unique data	4661	4796
Refinement method	Full-matrix least-squares on $ F ^2$	Full-matrix least-squares on $ F ^2$
<i>R</i> _{merg}	0.038	0.0648
<i>R</i> indexes [<i>I</i> > 2 <i>S</i> (<i>I</i>)]	$R_1 = 0.0301^a$, $wR_2 = 0.0750^b$	$R_1 = 0.0738^a$, $wR_2 = 0.1417^b$
Goodness of fit (<i>S</i> _{obs})	1.023	1.049
No. of variables	444	442
Largest difference map hole and peak (eÅ ⁻³)	-0.668 and 0.726	-1.276 and 1.180

^a $R_1 = \sum |F_0| - |F_c| / \sum |F_0|$; ^b $wR_2 = \{\sum [w(F_0^2 - F_c^2)^2] / \sum [w(F_0^2)^2]\}^{1/2}$. $w = 1/[S^2(F_0)^2 + (aP)^2 + bP]$, $P = [\max. (F_0^2, 0) + 2(F_c^2)]/3$, where $a = 0.0423$ and $b = 2.4339$ for **I** and $a = 0.0715$ and $b = 0.0$ for **II**.

three distinct sets depending on the bonding. Thus, the shorter Mo–O distances of 1.801(4)–1.725(4) corresponds to Mo–O_(terminal), and the medium distances of 1.988(4)–1.966(4) correspond to Mo–O_(bridging) and the longer distances of 2.181(4)–2.358(4) Å correspond to M–O_(bridging involving P) respectively. Similar bond distances have been observed earlier.^{6,12–19} The O–Mo–O bond angles are in the range 69.28(14)–172.52(17) $^{\circ}$ (average = 103.6 $^{\circ}$). The Mo atoms form six bonds with two distinct P atoms with average Mo–O–P bond angles of 128.1 $^{\circ}$. Each P atom makes three connections with Mo and possesses one P–O terminal bond with an average P–O distance of 1.541 Å. O–P–O bond angles have an average value of 109.5 $^{\circ}$, confirming the tetrahedral nature of the phosphate units. All the bond distances and angles are as expected for this type of bonding. Selected bond distances are listed in table 2.

As in **I**, the asymmetric unit of **II** also consists of 49 non-hydrogen atoms, of which 30 atoms belong to the pentamolybdatobisphosphate and the remaining belong to four molecules of water and three molecules of completely protonated 1,2-diaminopropane molecules. Various bond distances and angles are similar to those of **I** and not much deviation in the parameters has been observed. Selected bond distances are listed in table 3.

Structures of both **I** and **II** consist of a cluster of five octahedral Mo atoms. The octahedrons are assembled in such a way that they are connected through four common edges and one common corner to form a five-membered ring (figure 4). Thus, for **I**, Mo(1) and Mo(5), Mo(5) and Mo(3), Mo(3) and Mo(2), Mo(1) and Mo(4) share edges and Mo(4) and Mo(2) share a corner and for **II**, Mo(1) and Mo(3), Mo(3)

Table 3. Selected bond distances for **II** [(C₃N₂H₁₂)₃[P₂Mo₅O₂₃]·4H₂O]

Bond	Distance (Å)	Bond	Distance (Å)
Mo(1)–O(1)	1.714(12)	Mo(4)–O(18)	1.727(11)
Mo(1)–O(2)	1.744(12)	Mo(4)–O(10)	1.916(11)
Mo(1)–O(3)	1.899(12)	Mo(4)–O(15)	1.960(11)
Mo(1)–O(4)	1.928(11)	Mo(4)–O(16)	2.261(11)
Mo(1)–O(5)	2.233(12)	Mo(4)–O(12)	2.308(10)
Mo(1)–O(6)	2.380(11)	Mo(5)–O(19)	1.678(11)
Mo(2)–O(7)	1.693(12)	Mo(5)–O(20)	1.735(12)
Mo(2)–O(8)	1.750(12)	Mo(5)–O(3)	1.937(11)
Mo(2)–O(9)	1.909(11)	Mo(5)–O(9)	1.949(12)
Mo(2)–O(10)	1.945(10)	Mo(5)–O(21)	2.236(11)
Mo(2)–O(11)	2.258(10)	Mo(5)–O(11)	2.411(10)
Mo(2)–O(12)	2.265(11)	P(1)–O(22)	1.501(12)
Mo(3)–O(14)	1.707(12)	P(1)–O(21)	1.527(12)
Mo(3)–O(13)	1.716(11)	P(1)–O(6)	1.562(11)
Mo(3)–O(15)	1.911(11)	P(1)–O(12)	1.577(11)
Mo(3)–O(4)	1.955(12)	P(2)–O(23)	1.517(12)
Mo(3)–O(6)	2.183(11)	P(2)–O(5)	1.519(12)
Mo(3)–O(16)	2.392(11)	P(2)–O(11)	1.557(11)
Mo(4)–O(17)	1.705(11)	P(2)–O(16)	1.566(12)

Table 2. Selected bond distances for **I** [(C₄N₂H₁₂)₃[P₂Mo₅O₂₃]·H₂O]

Bond	Distance (Å)	Bond	Distance (Å)
Mo(1)–O(1)	1.710(4)	Mo(4)–O(17)	1.725(4)
Mo(1)–O(2)	1.716(4)	Mo(4)–O(10)	1.877(4)
Mo(1)–O(3)	1.940(4)	Mo(4)–O(4)	1.945(4)
Mo(1)–O(4)	1.943(4)	Mo(4)–O(19)	2.250(4)
Mo(1)–O(5)	2.205(4)	Mo(4)–O(5)	2.372(4)
Mo(1)–O(6)	2.349(4)	Mo(5)–O(20)	1.717(4)
Mo(2)–O(7)	1.923(4)	Mo(5)–O(21)	1.725(4)
Mo(2)–O(8)	1.703(4)	Mo(5)–O(3)	1.898(4)
Mo(2)–O(9)	1.717(4)	Mo(5)–O(15)	1.917(4)
Mo(2)–O(10)	1.942(4)	Mo(5)–O(16)	2.287(4)
Mo(2)–O(11)	2.268(4)	Mo(5)–O(6)	2.331(4)
Mo(2)–O(12)	2.345(4)	P(1)–O(19)	1.526(4)
Mo(3)–O(7)	1.908(4)	P(1)–O(23)	1.528(4)
Mo(3)–O(13)	1.722(4)	P(1)–O(6)	1.555(4)
Mo(3)–O(14)	1.701(4)	P(1)–O(12)	1.560(4)
Mo(3)–O(15)	1.966(4)	P(2)–O(22)	1.515(4)
Mo(3)–O(16)	2.358(4)	P(2)–O(11)	1.530(4)
Mo(3)–O(12)	2.181(4)	P(2)–O(16)	1.550(4)
Mo(4)–O(18)	1.711(4)	P(2)–O(5)	1.562(4)

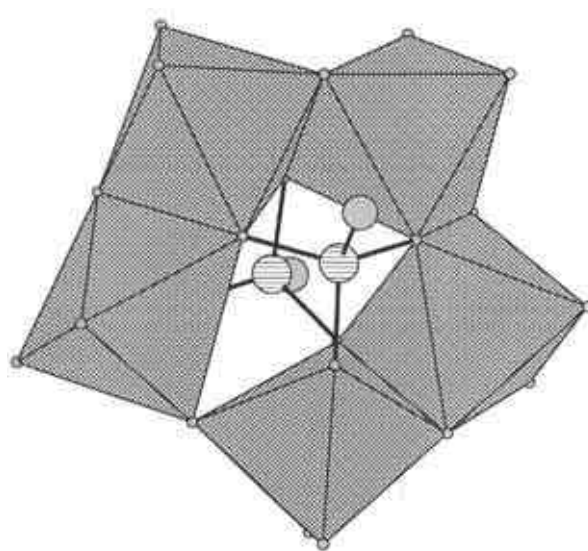


Figure 4. The pentamolybdatobisphosphate ion, [P₂Mo₅O₂₃]⁶⁻. Note that two Mo octahedra share a corner and the remaining are connected through their edges.

Table 4. Important hydrogen bond interactions in **I** $[(\text{C}_4\text{N}_2\text{H}_{12})_3][\text{P}_2\text{Mo}_5\text{O}_{23}] \cdot \text{H}_2\text{O}$, and **II** $[(\text{C}_3\text{N}_2\text{H}_{12})_3][\text{P}_2\text{Mo}_5\text{O}_{23}] \cdot 4\text{H}_2\text{O}$.

D–H...A moiety	D–H	H...A	D...A	D–H...A
I				
N(2)–H(8)...O(18)	0.90	2.52	3.327(8)	150
N(11)–H(14)...O(9)	0.90	2.56	3.457(8)	174
N(21)–H(25)...O(4)	0.90	2.22	2.934(6)	136
N(22)–H(31)...O(19)	0.90	1.95	2.785(6)	153
N(22)–H(32)...O(11)	0.90	1.96	2.820(6)	160
C(1)–H(3)...O(100)	0.97	2.44	3.240(9)	140
C(2)–H(5)...O(23)	0.97	1.83	2.761(7)	160
C(4)–H(11)...O(22)	0.97	1.64	2.593(7)	166
C(12)–H(17)...O(21)	0.97	1.82	2.785(7)	171
C(12)–H(18)...O(13)	0.97	1.90	2.783(7)	150
C(13)–H(22)...O(100)	0.97	2.52	3.298(9)	138
C(14)–H(23)...O(20)	0.97	2.02	2.874(7)	146
C(14)–H(24)...O(23)	0.97	1.72	2.652(7)	161
C(21)–H(28)...O(10)	0.97	2.50	3.475(7)	179
C(22)–H(30)...O(18)	0.97	2.56	3.409(8)	146
C(23)–H(34)...O(4)	0.97	2.31	3.094(8)	138
II				
N(1)–H(1)...O(22)	0.89	1.88	2.71(2)	155
N(1)–H(2)...O(23)	0.89	2.08	2.86(2)	145
N(1)–H(3)...O(300)	0.89	2.17	3.06(2)	178
N(2)–H(10)...O(4)	0.89	2.10	2.87(2)	144
N(2)–H(11)...O(300)	0.89	2.08	2.97(2)	176
N(2)–H(12)...O(200)	0.89	2.13	2.92(2)	147
N(11)–H(13)...O(10)	0.89	1.95	2.80(2)	161
N(11)–H(14)...O(100)	0.89	1.99	2.85(2)	160
N(11)–H(15)...O(18)	0.89	2.46	3.23(2)	145
N(12)–H(22)...O(22)	0.89	2.08	2.93(2)	160
N(12)–H(23)...O(7)	0.89	2.54	3.26(2)	138
N(12)–H(24)...O(15)	0.89	1.94	2.80(2)	163
N(21)–H(26)...O(11)	0.89	2.34	3.06(2)	138
N(21)–H(26)...O(23)	0.89	2.24	3.06(2)	153
N(21)–H(27)...O(100)	0.89	1.92	2.79(2)	168
N(22)–H(34)...O(2)	0.89	2.02	2.90(2)	172
N(22)–H(35)...O(23)	0.89	1.84	2.72(2)	168
N(22)–H(36)...O(400)	0.89	2.02	2.90(3)	170
C(1)–H(5)...O(18)	0.97	2.38	3.27(2)	153
C(11)–H(17)...O(17)	0.97	2.50	3.28(2)	137
C(23)–H(32)...O(2)	0.96	2.46	3.31(2)	148

and Mo(4), Mo(4) and Mo(2), Mo(2) and Mo(5) share edges and Mo(1) and Mo(5) share a corner. In both the cases, this five-membered ring is capped on either side by the phosphate tetrahedra through three basal oxygen atoms and possesses one terminal oxygen atom completing the pentamolybdate-bisphosphate as shown in figure 4. The molecular packing diagrams of **I** in the *ac* plane and for **II** in the *ab* plane are shown in figures 5 and 6.

Owing to the presence of organic amine molecules and the molecular nature of the compounds, a

large number of hydrogen bond interactions have been observed. The majority of the interactions are between the terminal oxygen atoms of the pentamolybdate-bisphosphate and the hydrogen atoms of the amine molecule. Thus, N...O and C...O distances are in the range 2.79–3.46 Å and 2.59–3.47 Å, respectively with the majority of D–H...O bond angles $>150^\circ$. Similar hydrogen bond interactions have also been observed for **II** (figures 5 and 6). The important hydrogen bond interactions observed in **I** and **II** are listed in table 4.

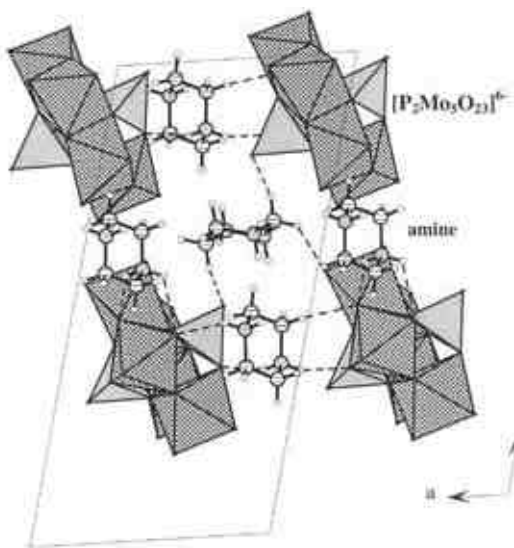


Figure 5. Packing diagram of **I** $[(C_4N_2H_{12})_3[P_2Mo_5O_{23}] \cdot H_2O]$, in the *ac* plane showing the arrangement of the pentamolybdatobisphosphate anions and the amine molecules. Water molecules are not shown. The dotted lines represent possible hydrogen bond interactions.

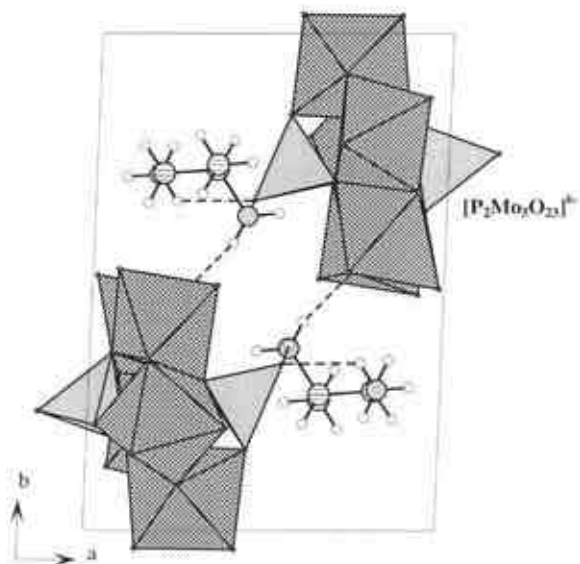


Figure 6. Packing diagram of **II** $[(C_3N_2H_{12})_3[P_2Mo_5O_{23}] \cdot 4H_2O]$, in the *ab* plane showing the arrangement of the pentamolybdatobisphosphate anions and the amine molecules. Water molecules are not shown. Dotted lines represent possible hydrogen bond interactions.

The hydrothermal method offers a convenient route for the synthesis of organic–inorganic hybrid compounds. The unique chemical features of the organic and inorganic components may complement each other in such materials to give rise to new solid-

state structures and, in some cases, composite structures. The organic component, generally amines, in many of the syntheses has been used extensively as charge-compensating, space-filling and structure-directing roles in the design of materials. In the present case, the amine molecules act as charge-balancing cations. The polyanions of the type described here have been formed in the pH range of 6–8, though the pentamolybdatobisphosphate anions have been stabilized recently even at a pH of 3.²¹ Though the synthesis has been carried out at relatively neutral pH (~7), the protonation of the organic amine molecules can be explained as originating due to the local concentration effects. Many examples of protonated organic amine species being formed during the synthesis of open-framework solids at basic pH are known.²⁶ In addition, the presence of ferrous chloride in the synthesis mixture also did not contribute to the reduction of the molybdenum centers, which indicates that local concentration effects are likely to play an important role in the formation of these phases. It has been observed that the acidic pH helps in obtaining larger yields of the Strandberg clusters.²¹ The present work clearly shows that it is possible to stabilize the pentamolybdatobisphosphate anions in the presence of charge-balancing organic cations. The pentamolybdatobisphosphate anion appears to stabilize in the presence of other organic amine molecules and we are presently continuing this theme.

CCDC-260875 and 260876 contain the supplementary crystallographic data for compounds **I** and **II** for this paper. These data can be obtained from the above, via www.ccdc.co.uk/conts/retrieving.html (or from Cambridge Crystallographic Data Centre, 12 Union Road, Cambridge CB2 1EZ, UK, FAX: +44-1223-336-033, e-mail: deposit@ccdc.cam.ac.uk.).

Acknowledgements

The authors thank the Council of Scientific and Industrial Research, Government of India for a research grant.

References

1. Pope M T and Muller A (eds) 2001 *Polyoxometalate chemistry: From topology via self-assembly to applications* (Dordrecht: Kluwer)
2. Hill C (ed.) 1998 *Chem. Rev.* **98** 1–390 (Special issue on polyoxometalates)
3. Pope M T and Muller A 1991 *Angew. Chem., Int. Ed. Engl.* **30** 34

4. Pope M T 1983 *Heteropoly and isopoly oxometalates* (Berlin: Springer)
5. Muller A, Kogerler P and Dress A M W 2001 *Coord. Chem. Rev.* **222** 193, and references therein
6. Strandberg R 1973 *Acta Chem. Scand.* **27** 1004
7. Ozeki T, Ichida H, Miyamae H and Sasaki Y 1988 *Bull. Chem. Soc. Jpn.* **61** 4455
8. Hori T, Himeno S and Tamada O 1992 *J. Chem. Soc., Dalton Trans.* 275
9. Shivaiah S, Arumuganathan T and Das S K 2004 *Inorg. Chem. Commun.* **7** 367
10. Souchay P 1963 *Polyanions et Polycations* (Paris: Gauthier Villers)
11. Khan M I, Chen Q and Zubieta J 1993 *Inorg. Chem.* **32** 2924
12. Jeannin Y P 1998 *Chem. Rev.* **98** 51, and references therein
13. Holscher M, Englert U, Zibrowius B and Holderich W F 1994 *Angew. Chem., Int. Ed. Engl.* **33** 2491
14. Zubieta J 1999 *Angew. Chem., Int. Ed. Engl.* **38** 2638, and references therein
15. Krebs B, Lindqvist B and Pohlmann H 1989 *Z. Kristallogr.* **186** 233
16. Li Y F, Cui W, Zhu G D, Qiu S L, Fang Q R and Wang C L 2003 *Chem. J. Chinese Univ.* **24** 394
17. Aranzabe A, Wery A S J, Martin S, Guiterrz-Zorrilla J M, Luque A, Martinez-Ripoll M and Roman P 1997 *Inorg. Chim. Acta* **255** 35
18. Kwak W, Pope M T and Scully T F 1975 *J. Am. Chem. Soc.* **97** 5753
19. Stalick J K and Quicksall C O 1976 *Inorg. Chem.* **15** 1577
20. Lyxell D G and Strandberg R 1988 *Acta Crystallogr. C* **44** 1535
21. Kortz U, Marquer C, Thouvenot R and Nierlich M 2003 *Inorg. Chem.* **42** 1158
22. Chakrabarti S and Natarajan S 2002 *Crystal Growth Design* **2** 333
23. Feng P 2001 *Chem. Commun.* 1668
24. Sheldrick G M 1994 *SADABS Siemens Area Detector Absorption Correction Program*, University of Göttingen, Gottingen, Germany
25. Sheldrick G M 1997 *SHELX-97 Program for Crystal Structure Solution and Refinement*, University of Gottingen, Gottingen, Germany
26. Vaidhyanathan R, Natarajan S and Rao C N R 1999 *J. Mater. Chem.* **9** 2789